AGU PUBLICATIONS

Geophysical Research Letters

RESEARCH LETTER
10.1002/2016GL071185

Key Points:
- Cloud top radiative cooling is significantly correlated with cloud updrafts for stratocumulus over east Pacific and northeast Atlantic
- Based on this relationship, we quantify the cloud updrafts by stratocumulus cloud top radiative cooling
- This quantification scheme can be utilized by satellite remote sensing and model parameterization of cloud base updraft

Supporting Information:
- Supporting Information S1
- Table S1

Correspondence to:
Y. Zheng,
yzheng@atmos.umd.edu

Citation:
Zheng, Y., D. Rosenfeld, and Z. Li (2016), Quantifying cloud base updraft speeds of marine stratocumulus from cloud top radiative cooling, *Geophys. Res. Lett.*, *43*, doi:10.1002/2016GL071185.

Received 19 JUL 2016
Accepted 21 OCT 2016
Accepted article online 22 OCT 2016

©2016. American Geophysical Union. All Rights Reserved.

Quantifying cloud base updraft speeds of marine stratocumulus from cloud top radiative cooling

Youtong Zheng[1], Daniel Rosenfeld[2], and Zhanqing Li[1]

[1]Department of Atmospheric and Oceanic Science and Earth System Science Interdisciplinary Center, University of Maryland, College Park, Maryland, USA, [2]Institute of Earth Sciences, Hebrew University of Jerusalem, Jerusalem, Israel

Abstract Marine stratocumulus clouds play a significant role in the Earth's radiation budget. The updrafts at cloud base (W_b) govern the supersaturation and therefore the activation of cloud condensation nuclei, which modifies the cloud and precipitation properties. A statistically significant relationship between W_b and cloud top radiative cooling rate (CTRC) is found from the measurements of the Department of Energy's Atmospheric Radiation Measurement Mobile Facility on board a ship sailing between Honolulu and Los Angeles. A similar relation was found on Graciosa Island but with greater scatter and weaker correlation presumably due to the island effect. Based on the relation, we are able to estimate the cloud base updrafts using a simple formula: $W_b = -0.44 \times \mathrm{CTRC} + 22.30 \pm 13$, where the W_b and CTRC have units of cm/s and W/m^2, respectively. This quantification can be utilized in satellite remote sensing and parameterizations of W_b in general circulation models.

1. Introduction

Updrafts at cloud base (W_b) govern the supersaturation and therefore the activation of cloud condensation nuclei, which further controls the cloud and precipitation properties [*Rogers and Yau*, 1996; *Twomey*, 1959]. Measuring W_b is essential for both understanding the cloud physics and for isolating the aerosol-mediated effect on cloud properties and, consequently, for unlocking anthropogenic climate forcing in combination with climate models [*Donner et al.*, 2016]. Unfortunately, observation of updraft has been most difficult and uncertain. Current approaches of observing updrafts are limited to in situ measurements by towers and aircraft and remote sensing by vertically pointing radars and lidars [*Ghate et al.*, 2010; *Kollias et al.*, 2001]. Both of them are high-cost measurements over very limited areas.

Here we address this shortcoming by developing a satellite-based methodology for retrieving W_b for marine stratocumulus (MSc) over large areas. *Zheng et al.* [2015] and *Zheng and Rosenfeld* [2015] have already developed such a method for satellite estimation of W_b of boundary layer (BL) convective clouds, by using surface and BL physical parameters. This relies on the dominant role of surface heating in driving the convection in boundary layer topped by convective clouds. Larger sensible surface heat flux and higher cloud bases were found to be associated with larger W_b. Unlike convective clouds, which are propelled mainly by surface heating, MSc is propelled primarily by cloud top radiative cooling (CTRC) [*Lilly*, 1968; *Moeng et al.*, 1996]. A relationship between W_b and CTRC may thus exist which can serve as a basis for a simple approach of quantifying W_b for marine stratocumulus by using combined satellite measurements of cloud top temperature and vertical profiles of moisture above cloud tops using reanalysis data. We will exploit the approach by using island and ship-based observations of a large number of MSc clouds across the northeastern Atlantic and Pacific Oceans.

In the next section, we introduce the data sets used in this study, the methodology of cloud base updraft measurements, and the radiative transfer model. Results are presented in section 3, followed by a section giving the conclusion and the potential application.

2. Data and Methodology

2.1. Atmospheric Radiation Measurement Data

In this study, we used the data sets from both mobile observation facility and fixed-site facility of the Atmospheric Radiation Measurement (ARM) under the aegis of U.S. Department of Energy (DOE) during the Marine ARM Global Energy and Water Cycle Experiment-Cloud System Study-Pacific Cross-section

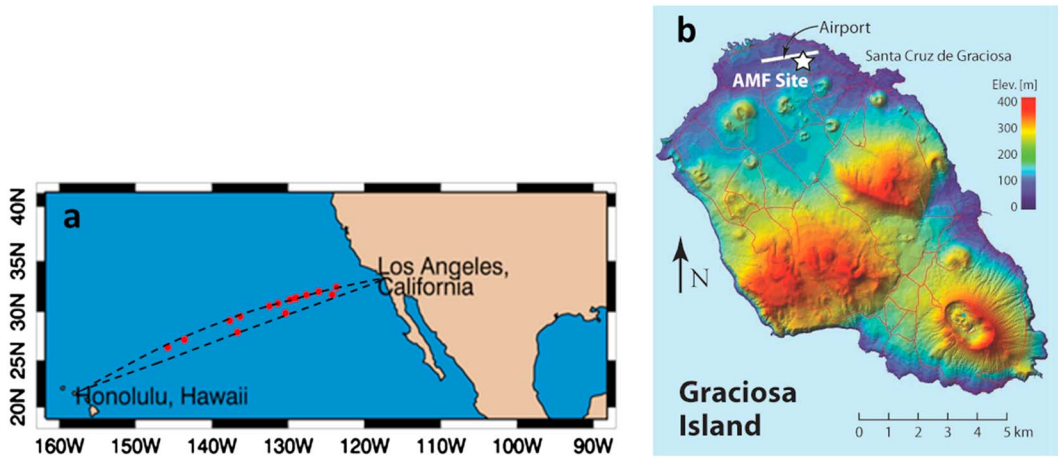

Figure 1. (a) Approximate track of MAGIC legs between California and Hawaii. The red dots mark the locations of the ship for the selected MAGIC cases. (b) Map of Graciosa Island showing the location of the AMF site, which is adapted from *Wood et al*. [2015].

Intercomparison Investigation of Clouds (MAGIC) campaign and on the island of Graciosa (GRW), Azores, in the northeastern Atlantic Ocean. W-band ARM Cloud Radar (WACR) was used to measure the cloud base updraft speed and cloud top height. The cloud base height was estimated by Vaisala Ceilometer (VCEIL). Radiosondes were launched at each location every 6 h, which were used to provide vertical profiles of temperature and humidity. Using the radiosonde data, lifting condensation level (LCL) was calculated from the bottom 25% of the planetary boundary layer [*Jones et al*., 2011]. Liquid water path (LWP) was derived from microwave radiometer (MWR). The ARM surface Meteorology System data at the GRW site provided the wind direction at 10 m above the ground level.

2.1.1. MAGIC Field Campaign

The MAGIC campaign lasted for nearly 1 year (from October 2012 to September 2013), providing high-resolution observations of clouds, aerosols, and marine boundary layer over the eastern Pacific region. The second ARM Mobile Facility, AMF2, was deployed on a cargo ship *Spirit* that made round trips between Los Angeles, California, and Honolulu, Hawaii, every 2 weeks (Figure 1a). The Marine W-band (95 GHz) ARM Cloud Radar Ship Correction Value-Added Product, which has corrected the Doppler velocity using the ship heave, was utilized to estimate the cloud base updraft speed.

2.1.2. Graciosa Island

The ARM Mobile Facility (AMF) was deployed near the north shore of Graciosa Island (June 2009 to December 2010) in the Azores Archipelago (Figure 1b). Although the island has a small area of ~60 km^2 and is assumed to provide observations with maritime behavior, the island effect should not be overlooked. Observations with southerly wind are exposed to effects by the underlying ground, and the island effect is amplified, whereas in northerly wind conditions the island effect is minimized. The effects include change in surface temperature compared to sea surface temperature and some topography that may induce changes in updraft speed.

2.2. Cloud Base Updrafts Measurements

Figure 2 presents a representative case on 11 September 2013 during the MAGIC campaign. W_b was computed based on WACR pixels of positive Doppler velocity during a 2 h time window and within the layer from cloud base to the half of cloud depth (red box in Figure 2b). We use the following equation $W_b = \sum N_i W_i^2 / \sum N_i W_i$, where N_i is the number of upward vertical velocity W_i ($W_i > 0$) pixels within the selected box at cloud base, to compute the cloud base updrafts. As described by *Zheng et al*. [2015], W_b is the cloud volume-weighted updraft. To ensure high-quality pixels with Doppler spectrum, width values below 0.1 m s^{-1} and signal-to-noise ratio values below −10 dB were removed. Here we assume that cloud droplets have negligible terminal velocities and use the cloud droplets to trace the vertical air motion, as our main interest is in nonprecipitating clouds. This assumption becomes invalid when drizzles or raindrops are present [*Kollias et al*., 2001]. To minimize the effect of raindrops, we perform the following two quality controls. First, we

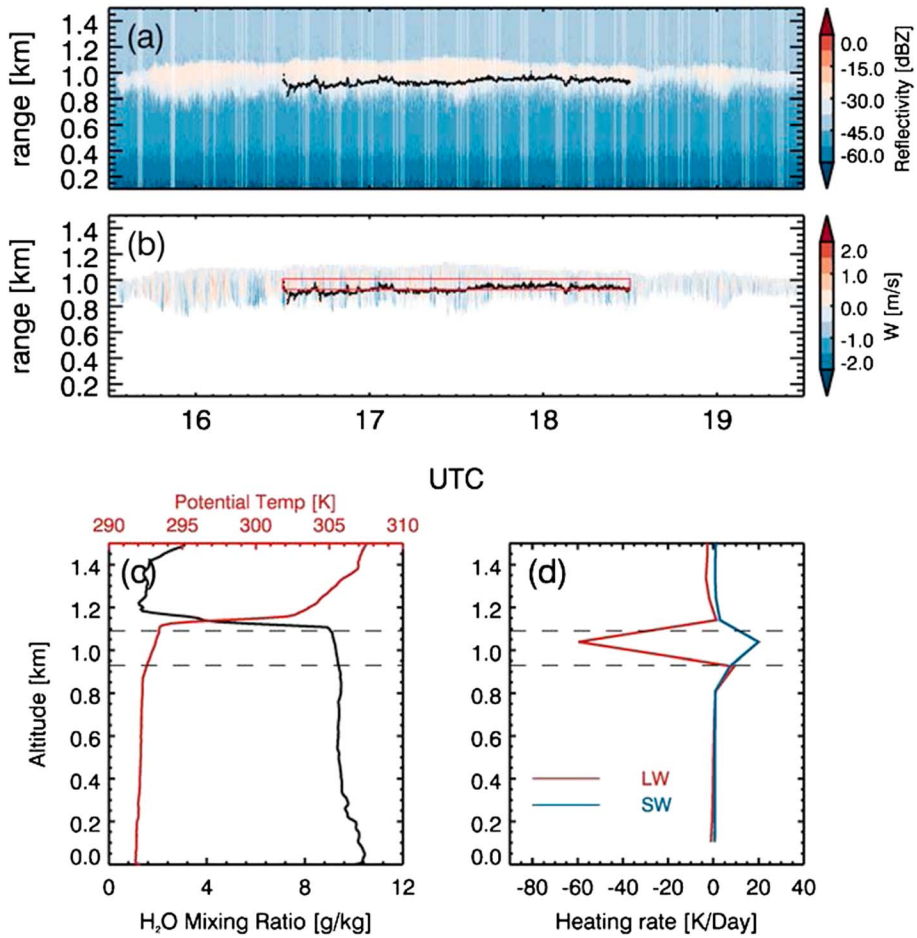

Figure 2. Height-time displays of WACR (a) reflectivity and (b) vertical velocity from WACR during MAGIC campaign. Black points denote the VCEIL-measured cloud base heights. The red box in Figure 2b denotes the height-time areas for cloud base window within which pixels are selected for computing W_b. Vertical profiles of (c) potential temperature (red line) and water vapor mixing ratio (black lines) as measured by the closest radiosondes, and (d) heating rates of longwave (red line) and shortwave (blue line) simulated by SBDART. The horizontal dashed lines mark the position of cloud base and top heights.

removed pixels with reflectivity larger than −17 dB*Z* [*Kogan et al.*, 2005]. Second, we remove the entire column of radar pixels in the height-time radar plot if the distance between the VCEIL-observed cloud base and WACR-observed rain base is larger than 200 m for that specific column (Figures S1a–S1e in the supporting information). Unlike VCEIL that is insensitive to raindrops and provides accurate cloud base heights, WACR is highly sensitive to raindrops and thus measures the bases of rain. The distance between the cloud base and rain base is considered as a measure of rain intensity. The threshold of 200 m is somewhat arbitrary, but we found that the measured W_b is not sensitive to this value (Figure S1f).

2.3. Retrieving Cloud Top Radiative Cooling Based On Radiative Model

The radiative transfer model used in this study is Santa Barbara discrete ordinates radiative transfer Atmospheric Radiative Transfer (SBDART) model. The vertical profiles of temperature, water vapor density, and ozone density are obtained from the closest radiosonde. The cloud base and top heights were determined using VCEIL and WACR, respectively. The LWP was obtained from the MWR. The cloud droplet effective radius was set as the default value of 8 μm in SBDART model. This may introduce some uncertainties, but sensitivity test results (Figure S2a) indicate that CTRC is not sensitive to cloud effective radius. An example of the vertical profiles of the longwave and shortwave heating rates during daytime as simulated by the SBDART is shown in Figure 2d. A strong longwave (LW) cooling occurs within the upper reaches of the cloud. A cloud behaves nearly as a blackbody with respect to longwave radiation and produces large upward

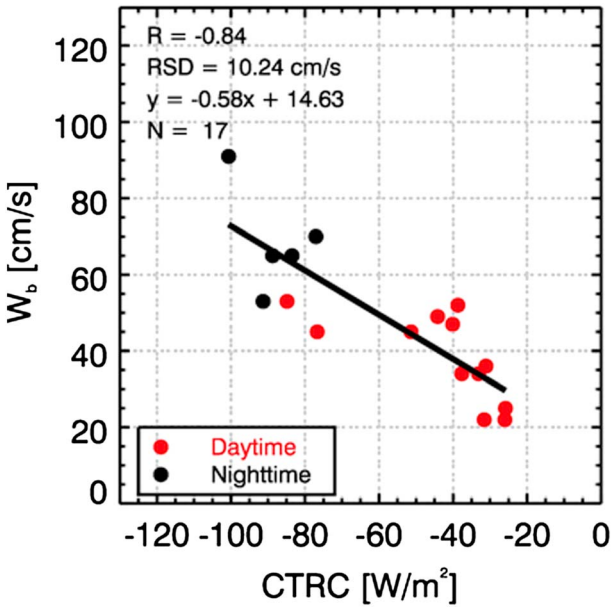

Figure 3. Variation of WACR-observed W_b with the cloud top radiative cooling over MAGIC campaign. The correlation coefficient (R), residual standard deviation (RSD), best fit regression equation, and case numbers (N) are provided. The red and black points stand for the daytime and nighttime cases, respectively.

blackbody flux that significantly exceeds the downward radiation originating from the above atmosphere with lower temperature and humidity. The heat losses at cloud top due to infrared radiation are partially offset by cloud top solar heating during daytime. At the base of a cloud, the cloud is typically slightly heated when the downward flux is exceeded by the flux from below. In this study, CTRC is quantified by integrating the heating rate through the entire cloud layer. The CTRCs for all the cases analyzed in this study are tabulated in Table S1. Each case corresponds to a 2 h segment of measurements. Assuming a BL wind speed of ~5 m/s, 2 h correspond to 36 km in length, which corresponds to a spatial scale of ~1000 km^2.

2.4. Case Selection

Cases with nonprecipitating stratocumulus were selected. The selection criteria were as follows: (1) The stratocumulus has to be full cloudy with VCEIL-measured cloud fraction larger than 90% during the 2 h segment. (2) Typically, the stratocumulus cloud top is radiatively cooled so that an inversion layer is present, capping the cloud. Therefore, cases with distance between cloud top and inversion layer larger than 200 m will be excluded to assure MSc identification. (3) The clouds must not precipitate significantly. Strong precipitation, for one part, distorts the vertical velocity measurements by WACR and for the other part may modify the thermodynamic structure that is not accounted for in radiative transfer simulations. If considerable precipitation is present, the quality control processes (removing pixels with reflectivity > -17 dBZ and distance between cloud base and rain base exceeds 200 m) will remove most radar pixels at the cloud base. Therefore, cases are identified as precipitating clouds and will be excluded if the ratio of the number of remaining radar pixels with positive vertical velocity after quality controls (N_{use}) to the total number of pixels (N_{tot}) within the cloud base window (red box in Figure 2b) is less than 5%. (4) Only single-layer clouds were selected by WACR. A total of 53 cases in GRW and 17 cases in MAGIC was selected. There are two reasons for the small samples in MAGIC. First, four months measurements (12 January to 9 May 2013) are missing due to the dry dock scheduled for the ship during the MAGIC campaign. Second, along transect of the ship *Spirit*, cloud regimes vary from stratocumulus near Los Angeles to cumulus near Honolulu [*Zhou et al.*, 2015]. Stratocumulus cases can only be found in the northern part of this transect (red points in Figure 1a).

3. Results

3.1. W_b-CTRC Relation Over MAGIC

Figure 3 shows the variation of WACR-measured W_b with CTRC over the MAGIC campaign. A statistically significant ($R = -0.84$) and tight (residual standard deviation, RSD, is 10 cm/s) relationship is present. The result is consistent with a dominant role for CTRC in driving the updrafts by virtue of enhancing the convective instability of the marine BL. The daytime cases (red) are characterized by weaker CTRCs than nighttime ones (black) due to solar absorption offsetting part of the LW cooling at cloud tops, as revealed in Table S1.

3.2. The Island Effect on the GRW Island

Unlike the MAGIC field campaign where the measurements were made over open ocean, the measurements on GRW island suffer from island effect. Either surface heating or orographic uplifting may produce additional

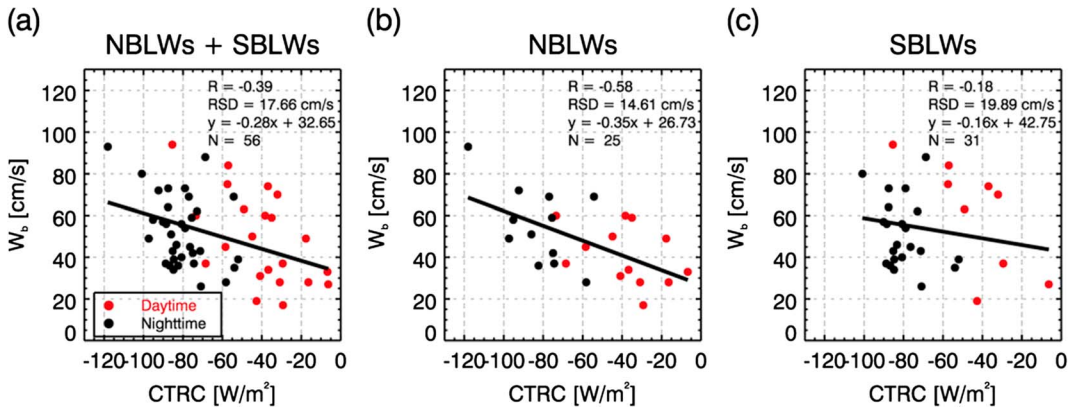

Figure 4. Variation of WACR-observed W_b with the cloud top radiative cooling rate on GRW island for (a) all cases, (b) NBLWs cases, and (c) SBLWs cases. The red and black points stand for the daytime and nighttime cases, respectively.

vertical velocity and disturb the relation. As shown by Figure 4a, W_b correlates with CTRC over the GRW site with much weaker correlation coefficient and greater scatter. As noted in section 2, island effect in GRW is amplified when the BL winds come from the south. To elucidate the island effects, we divide the data sets into two groups based on BL wind direction: southerly BL winds (SBLWs) and northerly BL winds (NBLWs). Results in Figures 4b and 4c show that the W_b and CTRC are more strongly correlated in NBLWs condition than in SBLWs, supporting the likelihood that the sensitivity of W_b to CTRC depends greatly on the island effect. Compared with the result from MAGIC, the scatter is much greater even for the NBLWs cases. There are two possible reasons. First, the cliffs to the north of the AMF site may bring additional upward wind in NBLWs condition, which adds noise to the relationship. Second, considering the small range of the W_b (20–100 cm/s), any island disturbance will considerably affect the relation, even if such disturbance is minimized in NBLWs condition. The evidence that island surface heating increases W_b and affects the W_b-CTRC relationship is presented in Figure S3, which shows stronger W_b of GRW cases for a given CTRC than their MAGIC counterparts during daytime. This enhanced W_b on GRW during daytime with lower values of CTRC reduces the sensitivity of W_b to CTRC. The slope of best fit linear equation decreases from 0.58 on MAGIC to 0.35 on GRW. Despite the disturbances from island effects, when we combine the data sets of GRW in NBLWs condition and MAGIC, the relationship still holds, with a correlation coefficient of −0.68 and RSD of ~13 cm/s (Figure 5a). Such relationship becomes more scattered when we add the removed precipitating cases (Figure S4a), suggesting that this relationship is susceptible to the effects of precipitation.

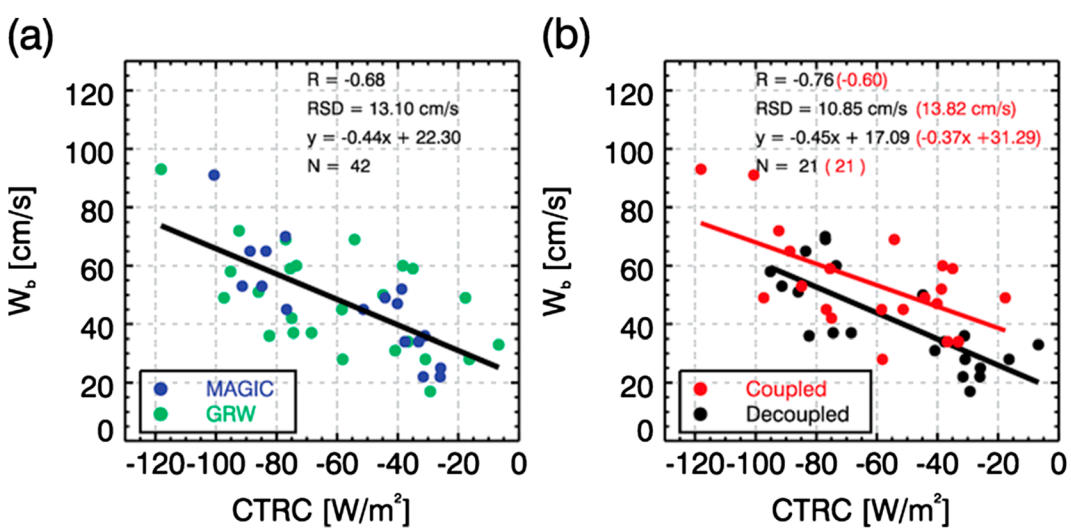

Figure 5. Variation of W_b with cloud top radiative cooling for MAGIC and GRW cases. The cases are color-coded based on (a) locations and (b) coupling state. In Figure 5a, the blue and green dots represent the MAGIC and GRW cases, respectively. In Figure 5b, the black and red dots/values represent the decoupled and coupled cases, respectively.

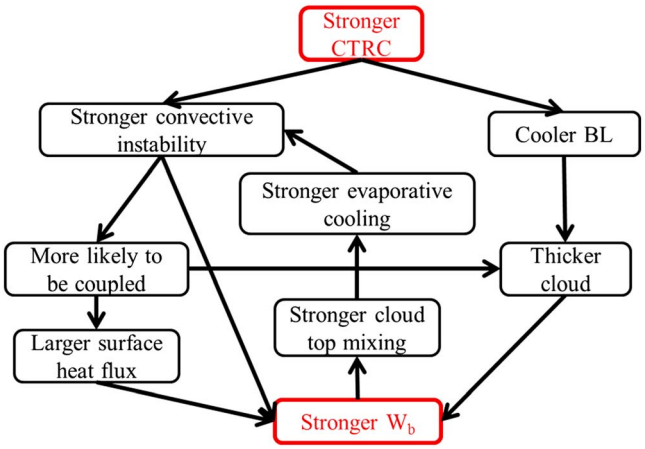

Figure 6. Conceptual diagram illustrating how CTRC regulates the W_b in stratocumulus clouds. This control of W_b by CTRC is one pathway of a more complicated system that involves numerous interactions and feedbacks, as noted by *Wood* [2012].

Figure 5b shows the CTRC-W_b relationship in coupled and decoupled BLs. Following *Jones et al.* [2011], we use 0.15 km of difference between H_b and LCL as the threshold to discriminate between coupled and decoupled cases. In decoupled regimes, clouds are less likely to be affected by the underlying surface. Two salient features are present in Figure 5b. First, the updrafts for coupled cases are systematically stronger by 8 to 13 cm/s than for decoupled cases. In a coupled BL, a steady state is maintained by both the "pull" effect of CTRC and "push" effect of heat flux from surface [*Wood*, 2012]. The push effect produces additional energy for the convection. Second, the relation in decoupled condition is tighter than in coupled state primarily due to the reduced perturbations from surface effects. This feature is especially prominent on GRW, where the W_b-CTRC correlation for decoupled cases ($R = -0.68$ and RSD = 11.65 cm/s) is considerably higher than for coupled cases ($R = -0.50$ and RSD = 16.16 cm/s) shown in Figure S5a.

3.3. CTRC: The Main Driver of Updrafts

Figure 6 illustrates the means by which CTRC regulates the W_b. Stronger CTRC enhances the W_b first by increasing the convective instability. With stronger convective instability, the turbulent eddies are intense enough to penetrate down into the lower subcloud layer to couple with the surface. For one part, in a coupled BL, surface heat flux provides additional push to promote stronger W_b. For another, being coupled, the stratocumulus gains more moisture supply from the surface than uncoupled stratocumulus and grows in thickness. In the meantime, CTRC cools the cloud layer, thickening the clouds via reducing the moisture holding capacity of air. Such dependence of cloud depth on CTRC is found in this study ($R = -0.49$ in Figure S6). Thicker clouds provide stronger latent heating, which further accelerate air parcels. These combined effects cause stronger vertical velocities in clouds, leading to stronger cloud top mixing. The entrainment of dry air could potentially result in considerable evaporative cooling of cloud droplets in cloud top, further enhancing the convective instability and forming a positive feedback. Of course, the entrainment will also dry the BL and prevent the cloud from growing too thick, which serves as a negative feedback to maintain a steady state for this dynamic system.

4. Conclusions

In this study, a simple relation is found between the updraft at cloud base (W_b) and radiative cooling at cloud top for MSc clouds using comprehensive ground-based observations from the DOE/ARM over the MAGIC oceanic campaign and GRW site. The major conclusions are as follows:

1. The relation between W_b and CTRC provides a simple means of quantifying the W_b using the formula: $W_b = \mathrm{m} \times \mathrm{CTRC} + \mathrm{b} \pm 13$, in which $m = -0.44 \pm 0.07$ and $b = 22.30 \pm 4.75$ (Figure 5a). The units of W_b and CTRC are cm/s and W/m^2, respectively.
2. On GRW, by removing the SBLWs and coupled cases, we minimize the island effects and significantly improve the R of W_b-CTRC relation from -0.39 to -0.68. This fact, together with the statistically significant correlation ($R = -0.84$) over MAGIC, attests to the robustness of this relation for MSc over open oceans.
3. This relation can be used for satellite remote sensing of W_b. The computation of CTRC requires the atmospheric soundings and observations of cloud properties (e.g., cloud base height, cloud top height, cloud optical depth, and cloud droplet effective radius) as the inputs of the radiative transfer simulation. All of these inputs are available from satellite with different degrees of uncertainties. The sensitivity tests (Figure S2) show that the CTRC is not sensitive to the cloud effective radius and cloud optical depth. Theoretically,

the CTRC is most sensitive to the cloud top temperature and overlying moisture. It has been a mature practice of retrieving cloud top temperature by satellite with reliable accuracy.

4. The parameterization of vertical velocity has long been recognized as a core issue in numerical weather simulations. This situation might be enlightened by the quantification scheme proposed in this study.

Acknowledgments
The study was supported by the NOAA's JPSS program and NWS program (NA15NWS4680011) and the Department of Energy (DOE) Office of Science (BER) Atmospheric System Research Program (DE-SC0007171). The ground-based data in this study are available from website of ARM Climate Research Facility (www.archive.arm.gov/data).

References

Donner, L. J., T. A. O'Brien, D. Rieger, B. Vogel, and W. F. Cooke (2016), Are atmospheric updrafts a key to unlocking climate forcing and sensitivity?, *Atmos. Chem. Phys. Discuss.*, *2016*, 1–13.

Ghate, V. P., B. A. Albrecht, and P. Kollias (2010), Vertical velocity structure of nonprecipitating continental boundary layer stratocumulus clouds, *J. Geophys. Res.*, *115*, D13204, doi:10.1029/2009JD013091.

Jones, C., C. Bretherton, and D. Leon (2011), Coupled vs. decoupled boundary layers in VOCALS-REx, *Atmos. Chem. Phys.*, *11*(14), 7143–7153.

Kogan, Z. N., D. B. Mechem, and Y. L. Kogan (2005), Assessment of variability in continental low stratiform clouds based on observations of radar reflectivity, *J. Geophys. Res.*, *110*, D18205, doi:10.1029/2005JD006158.

Kollias, P., B. A. Albrecht, R. Lhermitte, and A. Savtchenko (2001), Radar observations of updrafts, downdrafts, and turbulence in fair-weather cumuli, *J. Atmos. Sci.*, *58*(13), 1750–1766.

Lilly, D. K. (1968), Models of cloud-topped mixed layers under a strong inversion, *Q. J. R. Meteorol. Soc.*, *94*(401), 292–309.

Moeng, C., W. Cotton, B. Stevens, C. Bretherton, H. Rand, A. Chlond, M. Khairoutdinov, S. Krueger, W. Lewellen, and M. MacVean (1996), Simulation of a stratocumulus-topped planetary boundary layer: Intercomparison among different numerical codes, *Bull. Am. Meteorol. Soc.*, *77*(2), 261–278.

Rogers, R., and M. K. Yau (1996), *A Short Course in Cloud Physics*, 3rd ed., Elsevier, New York.

Twomey, S. (1959), The nuclei of natural cloud formation. Part II: The supersaturation in natural clouds and the variation of cloud droplet concentration, *Geogr. Ann. Ser. A*, *43*(1), 243–249.

Wood, R. (2012), Stratocumulus clouds, *Mon. Weather Rev.*, *140*(8), 2373–2423.

Wood, R., M. Wyant, C. S. Bretherton, J. Rémillard, P. Kollias, J. Fletcher, J. Stemmler, S. De Szoeke, S. Yuter, and M. Miller (2015), Clouds, aerosols, and precipitation in the marine boundary layer: An arm mobile facility deployment, *Bull. Am. Meteorol. Soc.*, *96*(3), 419–440.

Zheng, Y., and D. Rosenfeld (2015), Linear relation between convective cloud base height and updrafts and application to satellite retrievals, *Geophys. Res. Lett.*, *42*, 6485–6491, doi:10.1002/2015GL064809.

Zheng, Y., D. Rosenfeld, and Z. Li (2015), Satellite inference of thermals and cloud base updraft speeds based on retrieved surface and cloud base temperatures, *J. Atmos. Sci.*, *72*(6), 2411–2428.

Zhou, X., P. Kollias, and E. R. Lewis (2015), Clouds, precipitation, and marine boundary layer structure during the MAGIC field campaign, *J. Clim.*, *28*(6), 2420–2442.